



## Post-collisional lamprophyric event in Sierra Norte, Córdoba, Argentina: Mineralogical, geochemical and isotopic characteristics

M.S. O'Leary<sup>a,\*</sup>, R. Lira<sup>b</sup>, M.J. Dorais<sup>c</sup>, C.C.G. Tassinari<sup>d</sup>

<sup>a</sup> CONICET – CIMAR, Facultad de Ingeniería, Universidad Nacional del Comahue, Avenida Buenos Aires 1400, 8300 Neuquén, Argentina

<sup>b</sup> CONICET – Museo de Mineralogía "Dr. A. Stelzner", Universidad Nacional de Córdoba, Avenida Vélez Sarsfield 299, 5000 Córdoba, Argentina

<sup>c</sup> Department of Geology, Brigham Young University, Provo, UT 84602-4606, USA

<sup>d</sup> Centro de Pesquisas Geocronológicas, Instituto de Geociências, Universidade de São Paulo, Rua do Lago 562, CEP 05508-080, SP, Brazil

### ARTICLE INFO

#### Keywords:

Spessartites  
Post-collisional  
Petrology and geochemistry  
Sr-Nd-Pb isotopes  
Rb/Sr age  
Sierra Norte  
Argentina

### ABSTRACT

Over 20 lamprophyre dykes, varying in width between a few centimeters and several meters, have been identified in central Sierra Norte – Eastern Pampean Ranges, Córdoba, Argentina. Their mineralogy and chemistry indicate that they are part of the calc-alkaline lamprophyres clan (CAL). They contain phenocrysts of magnesiohornblende ± augite set in a groundmass of magnesiohornblende, calcic-plagioclase, alkali feldspar, and opaque minerals, which designate them as spessartite-type lamprophyres. Alteration products include chlorite, calcite and iron oxides after mafic phenocrysts, though some are partially replaced by actinolite. Feldspars are replaced by carbonate and clay minerals.

The dykes are relatively primitive, and show restricted major element variation ( $\text{SiO}_2$  51.1–55.3 wt.%,  $\text{Al}_2\text{O}_3$  12–16.6 wt.%, total alkalies 1.5–4.7 wt.%), high Mg# (55–77), high Cr contents (27–988 ppm) and moderate to high Ni contents (60–190 ppm). Lamprophyre LILE (e.g., Rb averages 110 ppm, Sr 211–387 ppm, Ba 203–452 ppm) are high relative to HFSE (e.g., Ta 0.2–1.6 ppm, Nb 4–11 ppm, Y 17–21 ppm), and are enriched in LREE (30–70 times chondrite). They are characterized by relatively high  $^{208}\text{Pb}/^{204}\text{Pb}$  (38.8–39.9),  $^{207}\text{Pb}/^{204}\text{Pb}$  (~15.7), and  $^{206}\text{Pb}/^{204}\text{Pb}$  (18.7–20.1), combined with low ( $\epsilon_{\text{Nd}}$ ) (−4.69 to −1.52) and a relative moderately high ( $^{87}\text{Sr}/^{86}\text{Sr}$ ) of 0.7055–0.7074. The Rb-Sr whole rock isochron indicates an Early Ordovician age of  $485 \pm 25$  Ma. The calculated  $T_{\text{DM}}$  (1.7 Ga) suggests that these rocks appear to have originated from a reservoir that was created during a mantle metasomatism event related to the Pampean orogeny.

The Sierra Norte lamprophyres show affinities with a subduction-related magma in an active continental margin. Their geochemical and isotopic features suggest a multicomponent source, composed of enriched mantle material variably contaminated by crustal components. The lamprophyric suite emplacement occurred at the dawning stage of the Pampean orogeny, in a regional post-collisional extensional setting developed in the Sierra Norte-Ambargasta batholith (SNAB) in Early Ordovician times.

© 2008 Published by Elsevier Ltd.

### 1. Introduction

Lamprophyres are part of an heterogeneous group of porphyritic, mafic-ultramafic, volatile-rich, alkaline rocks, usually forming swarms of dykes, sills or pipe-clusters. Lamprophyres were recently considered as primary melts showing a broad spectrum of compositions in volcanic and plutonic rocks from a variety of geo-dynamic settings. Calc-alkaline lamprophyre clan constitutes a group of rocks that includes spessartites (hornblende-plagioclase), minettes (phlogopite-K-feldspar), vogesites (amphibole-K-feldspar), and kersantites (phlogopite-plagioclase), and are characteristically associated with plutonic and subvolcanic granitoid rocks

(Rock, 1987). Previous investigation aimed toward exploring the genetic hypothesis that calc-alkaline lamprophyres originate by contamination of basaltic or lamproitic magmas by continental crust or crustal melts (Rock, 1991).

Lamprophyre dykes are widespread in the Sierras Pampeanas of central Argentina (e.g., Daziano, 1986) but have been the subject of only a few detailed studies, like the Late Famatinian calc-alkaline lamprophyres of the Sierra de San Luis (López de Luchi, 1998; Sparisci and Brodkorb, 1998; Orozco and Ortiz Suárez, 2005). In the Sierra Norte-Ambargasta Ranges, previous works consist of brief petrographical descriptions of some lamprophyre dykes (Gordillo, 1955; Lucero, 1948, 1969; Sánchez Granel et al., 1967; Minería TEA, 1968; Miró, 2001). Kersantitic lamprophyres have been mentioned in the region between Chufia Huasi and La Puerta (Lucero, 1969) though in this area, only spessartite lamprophyres have been described petrographically.

\* Corresponding author. Tel./fax: +54 299 4485344.

E-mail address: [moleary@uncoma.edu.ar](mailto:moleary@uncoma.edu.ar) (M.S. O'Leary).

In this paper, we present petrographic, mineralogical, geochemical and isotopic information that suggests a complex source for these lamprophyres that, like other calc-alkaline lamprophyres, are associated with a post-collisional extensional event in a subduction-related setting during the final stages of the Pampean orogeny.

## 2. Geologic setting

The studied lamprophyre outcrops are located north of Córdoba province, between  $29^{\circ}28'$  –  $29^{\circ}58'$  S and  $64^{\circ}20'$  –  $64^{\circ}00'$  W, in the Sierra Norte-Ambargasta batholith (SNAB), the easternmost block of the Sierras Pampeanas system of Argentina.

In this area the SNAB consists of calc-alkaline, I-type granitoids representative of a Precambrian-Cambrian arc magmatism emplaced in a low grade metasedimentary sequence of Upper Precambrian age. The most primitive rocks of the magmatic sequence are diorite to tonalite microgranular enclaves that are included in the regionally dominant basement formed by granodiorite and monzogranite (GM, Lira et al., 1997) emplaced during Upper Precambrian to Cambrian times (Rapela et al., 1998; Sims et al., 1998; Koukharsky et al., 1999; Millone et al., 2003; Gromet et al., 2005). A differentiated dacitic to rhyolitic subvolcanic body (DR, Lira et al., 1997) called Cerro de los Burros (CDLB) by Lucero Michaut et al. (1995) intruded earlier granitoids; a precise age of this body is in debate, some authors indicate a Late Proterozoic age (Söllner et al., 2000; Millone et al., 2003), others a Late Cambrian age (Miró et al., 2005) and others propose an Early Cambrian age (Leal et al., 2003). Younger intrusions are represented by smaller units of more evolved miarolitic monzogranites of Cambrian age (ca. 525 Ma, Millone et al., 2003), thick tabular syenogranitic aplite bodies (ca. 500 Ma, Millone, 2004) and a considerable number of small Ordovician rhyolitic bodies and dykes (Rapela et al., 1991; Correa, 2003; O'Leary et al., 2006). Although most of these youngest intrusives have ages that, with errors, fall in the Ordovician, geologic setting and petrological and geochemical evidence indicate that they represent the closure of the Pampean orogeny. Only one intrusive event of peraluminous geochemistry, located in the southern part of the batholith, has been considered part of the Famatinian orogeny (i.e., the El Cerro granite; Baldo et al., 1998). A summarized time-event chart of major magmatic and mineralizing episodes in the Sierra Norte-Ambargasta ranges has been recently published by Franchini et al. (2005).

The lamprophyres analyzed in this study occur as dykes that cross-cut both the CDLB body and GM suite (Fig. 1), but more commonly intruded the latter. They have steep dips and randomly oriented strikes, thicknesses range from 0.1 to 5 m and variable lengths from tens to few hundred meters (O'Leary, 2004). These bodies lack chilled margins against their host rocks, and in some cases are associated with thin aplitic dykes.

## 3. Analytical methods

All samples were crushed to millimeter-scale grain size after removal of weathered rims, only fresh rock chips were selected and these chips were milled in a agate mortar; this material was used for major and trace element analyses which were determined by XRF on fused discs and pressed pellets at XRAL Laboratories (SGS-Canada). REE were determined by ICP-MS at Act-Labs (Canada). Mineral analyses were performed using a CAMECA SX50 electron microprobe in the Department of Geology of Brigham Young University, Provo, Utah, USA. All mineral phases were analyzed using an accelerating voltage of 15 kV, with a beam current of 10 nA and a focused beam of 10 mm in diameter. Natural standards are as follows: Na K $\alpha$  Jadeite, Mg K $\alpha$  MgO, Al K $\alpha$  Anorthite, Si and K K $\alpha$  Orthoclase, Ca K $\alpha$  Wollastonite, Ti K $\alpha$  Titanite, Mn K $\alpha$  Spessart-

tine, Fe K $\alpha$  Fayalite. For micro-analytic data, reduction was done based on the correction factors of Pouchou and Pichoir (1985).

The isotopic analyses were carried out at the Geochronological Research Center (CPGeo) of the Institute of Geosciences, University of São Paulo, Brazil. All samples were crushed to millimeter-scale grain size after removal of weathered rims and hand-picked under a stereoscopic magnifier. These chips were washed in purified water in an ultrasonic bath. Powered samples were used for Rb-Sr, Pb-Pb, and Sm-Nd determinations. The Pb-Pb analyses were made by acid digestion and Pb purification by carbonate ionic exchange using the NBS981 standard. The Rb-Sr and Sm-Nd analyses were prepared by standard methods according to the analytical procedures described by Kawashita modified (1972), and Sato et al. (1995), involving HF-HNO<sub>3</sub> dissolution plus HCl cation exchange. Analyzed samples had no visible solid residues after dissolution. The Sr isotopic ratios were normalized to  $^{86}\text{Sr}/^{88}\text{Sr} = 0.1194$ ; replicate analyses of  $^{87}\text{Sr}/^{86}\text{Sr}$  for the NBS987 standard gave a mean value of  $0.71028 \pm 0.00006$  ( $2\sigma$ ), the blanks for Sr were 5 ng. Nd ratios were normalized to a  $^{146}\text{Nd}/^{144}\text{Nd} = 0.72190$ . The averages of  $^{143}\text{Nd}/^{144}\text{Nd}$  for La Jolla and BCR-1 standards were  $0.511847 \pm 0.00005$  ( $2\sigma$ ) and  $0.512662 \pm 0.00005$  ( $2\sigma$ ), respectively. The blanks were less than 0.03 ng. Pb, Sr, and Nd isotopic analyses were carried out on a multicollector VG 354 Micromass and Finnigan-MAT 262 mass spectrometers. The isotopic data were regressed using the program of Ludwig (1999). The ages were calculated using the decay constants established in Steiger and Jäger (1977); for  $^{87}\text{Rb}$  was  $1.42 \times 10^{-11} \text{ yr}^{-1}$ ; for  $^{147}\text{Sm} = 6.54 \times 10^{-12} \text{ yr}^{-1}$ .

## 4. Petrology of the Sierra Norte lamprophyres

### 4.1. Petrography and mineralogy

The Sierra Norte lamprophyres are mesocratic to melanocratic rocks, hypidiomorphic, fine grained and microporphyratic to porphyritic with an aphanitic groundmass. In some cases banded structures indicating flow differentiation are present. Euhedral to subhedral phenocrysts include calcic amphibole, in some cases clinopyroxene and, more rarely, plagioclase; phenocrysts occur as individual grains and as radiating clusters forming a glomeroporphyratic texture. The groundmass consists of calcic amphibole, in addition to microlites of plagioclase and fine-grained potassium feldspar; both quartz and plagioclase occur as intergranular phases. Accessory minerals set in the groundmass include needles of apatite and opaque minerals (magnetite-hematite, bornite + chalcocite + chalcopyrite + covellite, and pyrite).

Many of the dykes are extensively altered (deuterically) and the primary minerals are largely replaced. Alteration products include chlorite, carbonate, epidote, and iron oxides after calcic amphiboles; clinopyroxenes and calcic amphiboles are occasionally transformed to a secondary amphibole, and feldspars are altered to clay minerals and sericite, epidote and carbonate. Locally, some dykes exhibit ocellar texture; ocelli are spheroidal to ovoidal aggregates, consisting of quartz and calcite, and are interpreted as globular structures mineralogically analogous to basaltic amygdalites (Rock, 1984). Xenocrystic quartz and feldspars occur in some samples, suggesting partial crustal contamination by assimilation of country rock.

Petrographic characteristics of the dykes are generally consistent with their inclusion in the lamprophyre family of rocks. In terms of the modal mineralogy, the dykes are spessartites (plagioclase, hornblende, augite) according to the IUGS classification (Streckeisen, 1979; Wooley et al., 1996).

Clinopyroxenes were identified in only one dyke (1391) and are classified as augite (Morimoto et al., 1988) with high TiO<sub>2</sub> and low

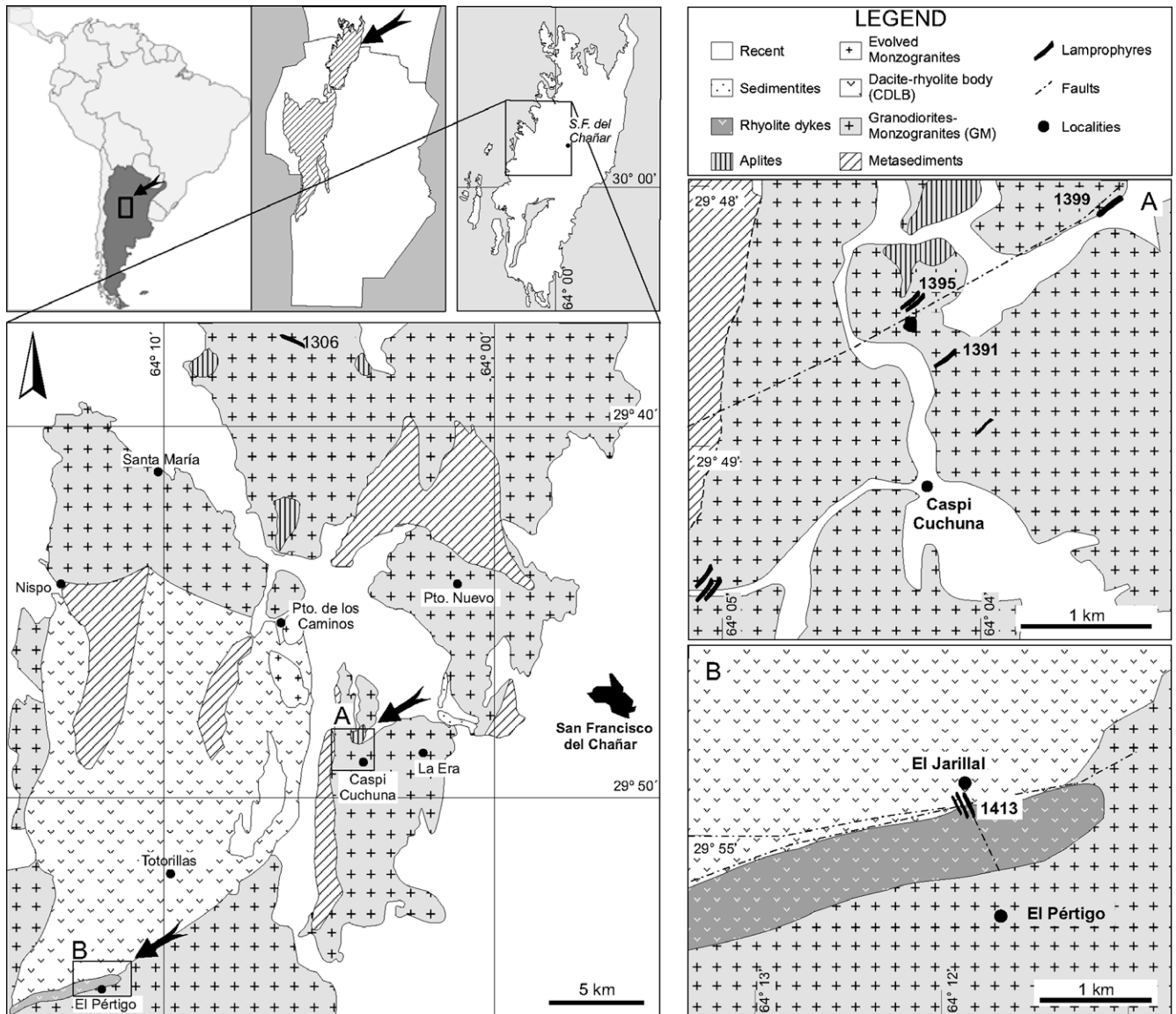


**Fig. 1.** Geological map of central Sierra Norte-Ambargasta in the eastern block of the Pampean Ranges of Argentina, showing the main rock types. A and B display the local geology of the sampled lamprophyres (they were enlarged for an easier identification).

$\text{NaO}_2$ . Representative analyses of mafic silicates are included in Table 1. Augites are in the compositional range of pyroxenes of calc-alkaline lamprophyres (CAL; Rock, 1987), and show an inverse relation between Mg# and the  $\text{TiO}_2$  and  $\text{Al}_2\text{O}_3$  contents. The relation between  $\text{Al}^{IV}$  and  $\text{Al}^{VI}$  contents in pyroxenes is used as an indicator of pressure conditions; in this case, the lamprophyric augites have a composition of high pressure pyroxenes, with  $\text{Al}^{IV}$  and  $\text{Al}^{VI}$  contents that range from 0.07 to 0.08 and 0.04 to 0.15, respectively (Bédard et al., 1988; Dorais, 1990).

The composition of phenocrysts of amphibole have little variation from one sample to another (structural formulae were calculated following the I.M.A. indications, Leake et al., 1997; Table 1); the lamprophyre dykes contain magnesiohornblende with very uniform composition, only one dyke contains edenite (sample 1399). The microprobe analyses indicate that the amphiboles are homogeneous and show no evidence of zoning or reaction with the melt. The cationic diagram  $\text{Ca} + \text{Al}^{IV}$  vs.  $\text{Si} + \text{Na} + \text{K}$  shows that the lamprophyric amphiboles present a compositional trend, starting with edenitic cores in sample 1399 and hornblende rims in

samples 1391–1399–1413, extending to actinolitic hornblendes in sample 1306 (Fig. 2). This evolutionary trend is distinguished by decreasing Al, Ti, Ca, Na and K, increasing Si, Fe and Mn, and almost constant Mg, Fe and Ti-tschermakitic and edenitic-type of substitutions (O'Leary, 2004), which suggest that the hornblendes, and probably the actinolitic hornblendes as well, are products of magmatic crystallization.

Additional evidence of primary equilibrium crystallization of amphiboles from the melt is from computed Mg# for the amphiboles using Bédard's (1988) equation ( $\text{Mg}\# \text{ amphibole} = 0.253125 \cdot \text{Mg}\# \text{ whole rock} + 0.5425$ ). The calculated values correspond closely to actual Mg#s of the amphiboles in the studied spessartites (Table 1). However, secondary  $\text{SiO}_2$ -poor actinolitic amphiboles after both primary amphiboles and clinopyroxenes were recognized.

Plagioclase from groundmass is relatively anorthitic ( $\text{An}_{56-76}$ ). Plagioclase in sample 1306 shows normal zoning with less calcic rims ( $\text{An}_{41-49}$ ), whereas sample 1391 plagioclase exhibits an inverse zoning with andesine–oligoclase core and labradorite rims.

**Table 1**

Representative electron microprobe compositions of mafic silicates of spessartite lamprophyres from central Sierra Norte-Ambargasta

	1306	1306	1306	1306	1306	1306	1399	1399	1399	1399	MUE1	MUE1	MUE1	1413	1413
	1	1	2	2	1	2	1	1	2	2	1	1	3	1	2
	Core	Rim	Core	Rim	Altered	Altered	Core	Rim	Core	Rim	Core	Rim	Intergr. cpx	Core	Core
<i>Amphiboles</i>															
SiO <sub>2</sub>	50.06	49.54	51.35	50.12	51.66	52.31	47.04	46.98	43.27	43.73	47.54	49.96	53.16	50.55	46.65
TiO <sub>2</sub>	0.08	0.17	0.29	0.20	0.10	0.09	0.92	0.95	2.33	2.27	1.66	0.94	0.50	0.29	1.37
Al <sub>2</sub> O <sub>3</sub>	5.49	5.85	4.31	5.54	4.09	3.75	7.23	6.91	9.63	9.78	7.41	5.37	3.25	4.35	6.59
FeO	14.35	13.41	13.21	12.95	12.48	11.54	11.03	11.31	10.63	10.91	12.87	13.03	10.09	15.49	18.56
MnO	0.40	0.41	0.46	0.48	0.39	0.37	0.27	0.31	0.21	0.22	0.29	0.39	0.34	0.48	0.58
MgO	13.75	14.38	15.28	14.93	15.14	15.94	15.09	14.63	14.30	14.36	15.12	15.26	17.14	13.39	11.19
CaO	12.36	12.14	11.75	11.65	12.56	12.36	10.70	10.89	11.03	11.10	11.12	10.53	11.81	11.77	11.48
Na <sub>2</sub> O	0.40	0.48	0.38	0.43	0.31	0.29	1.14	1.08	1.70	1.85	1.43	0.98	0.43	0.46	0.77
K <sub>2</sub> O	0.14	0.20	0.23	0.48	0.12	0.19	0.34	0.34	0.61	0.60	0.45	0.29	0.16	0.28	0.45
F	0.26	0.20	0.17	0.20	0.19	0.21	0.09	0.14	0.30	0.27	0.21	0.19	0.12	0.30	0.28
Cl	0.00	0.02	0.08	0.05	0.02	0.02	0.07	0.07	0.07	0.06	0.08	0.08	0.04	0.04	0.07
Total	97.28	96.79	97.50	97.03	97.05	97.07	93.92	93.62	94.07	95.15	98.16	97.02	97.04	97.39	97.99
F + Cl	0.11	0.09	0.09	0.09	0.08	0.09	0.06	0.08	0.14	0.13	0.11	0.10	0.06	0.34	0.35
Total	97.17	96.70	97.41	96.94	96.97	96.98	93.87	93.55	93.93	95.03	98.06	96.92	96.98	97.05	97.64
<i>Structural formulae based on O = 23</i>															
<sup>IV</sup> Si	7.448	7.369	7.430	7.288	7.599	7.552	7.008	7.054	6.534	6.536	6.891	7.262	7.614	7.411	6.932
<sup>IV</sup> Al	0.552	0.631	0.570	0.712	0.401	0.448	0.992	0.946	1.466	1.464	1.109	0.738	0.386	0.589	1.068
T site	8.000	8.000	8.000	8.000	8.000	8.000	8.000	8.000	8.000	8.000	8.000	8.000	8.000	8.000	8.000
<sup>VI</sup> Al	0.120	0.103	0.166	0.237	0.094	0.164	0.278	0.276	0.247	0.258	0.157	0.182	0.163	0.163	0.089
<sup>VI</sup> Tl	0.008	0.019	0.031	0.022	0.011	0.010	0.103	0.108	0.264	0.255	0.181	0.103	0.054	0.032	0.154
Fe <sup>3+</sup>	0.306	0.383	0.299	0.320	0.195	0.241	0.417	0.332	0.306	0.285	0.396	0.295	0.085	0.326	0.496
Mg	3.050	3.189	3.295	3.236	3.321	3.430	3.350	3.274	3.220	3.199	3.196	3.306	3.661	2.926	2.478
Fe <sup>2+</sup>	1.480	1.285	1.209	1.183	1.341	1.146	0.852	1.010	0.962	1.003	1.069	1.114	1.037	1.553	1.782
Mn	0.036	0.021	0.000	0.002	0.036	0.009	0.000	0.000	0.000	0.000	0.000	0.000	0.000	0.000	0.001
C site	5.000	5.000	5.000	5.000	4.998	5.000	5.000	5.000	5.000	5.000	5.000	5.000	5.000	5.000	5.000
Fe <sup>2+</sup>	0.000	0.000	0.091	0.073	0.000	0.005	0.106	0.080	0.074	0.076	0.094	0.175	0.087	0.019	0.032
Mn	0.014	0.031	0.056	0.058	0.012	0.037	0.033	0.039	0.027	0.028	0.035	0.048	0.042	0.059	0.072
Ca	1.970	1.934	1.799	1.815	1.974	1.912	1.709	1.753	1.784	1.778	1.726	1.640	1.812	1.849	1.829
Na	0.016	0.035	0.054	0.054	0.014	0.042	0.152	0.128	0.115	0.118	0.145	0.137	0.059	0.073	0.067
B site	2.000	2.000	2.000	2.000	1.996	2.000	2.000	2.000	2.000	2.000	2.000	2.000	2.000	2.000	2.000
Ca	0.000	0.000	0.000	0.000	0.005	0.000	0.000	0.000	0.000	0.000	0.000	0.000	0.000	0.000	0.000
Na	0.099	0.103	0.054	0.075	0.075	0.039	0.178	0.186	0.382	0.416	0.256	0.140	0.060	0.057	0.156
K	0.026	0.038	0.042	0.090	0.022	0.034	0.064	0.065	0.117	0.114	0.083	0.053	0.029	0.052	0.085
A site	0.125	0.141	0.096	0.165	0.103	0.074	0.243	0.250	0.499	0.530	0.339	0.193	0.089	0.110	0.241
Mg# <sup>a</sup>	<b>63.1</b>	<b>65.7</b>	<b>68.6</b>	<b>68.2</b>	<b>68.4</b>	<b>71.2</b>	<b>72.5</b>	<b>70.9</b>	<b>71.7</b>	<b>71.3</b>	<b>68.6</b>	<b>70.1</b>	<b>76.5</b>	<b>61</b>	<b>51.7</b>
Mg# <sup>b</sup>	<b>70.7</b>						<b>73.7</b>			<b>73.0</b>			<b>68</b>		
<i>Pyroxenes</i>															
							MUE1				MUE1			MUE1	
							1				2			2	
											(a)			(b)	
SiO <sub>2</sub>							52.05				52.01			52.17	
TiO <sub>2</sub>							0.37				0.54			0.57	
Al <sub>2</sub> O <sub>3</sub>							2.67				3.29			3.40	
FeO							5.82				5.80			6.47	
MnO							0.16				0.28			0.17	
MgO							16.50				16.26			16.41	
CaO							21.24				21.48			21.19	
Na <sub>2</sub> O							0.19				0.16			0.17	
K <sub>2</sub> O							0.01				0.02			0.01	
Total							99.02				99.85			100.56	
<i>Structural formulae based on O = 4</i>															
Si							1.922				1.921			1.926	
Al							0.078				0.079			0.074	
Fe															
T site							2.000				2.000			2.000	
Al							0.038				0.064			0.074	
Fe							0.108				0.179			0.199	
Ti							0.01				0.015			0.016	
Cr															
Mg							0.844				0.742			0.711	
Mn															
M1 site							1.000				1.000			1.000	
Mg							0.065				0.154			0.193	
Mn							0.005				0.008			0.005	
Ca							0.840				0.849			0.838	
Na							0.014				0.012			0.012	
K											0.001				
M2 site							0.924				1.024			1.048	
Wo							0.272				0.452			0.441	
En							0.553				0.489			0.466	
Fs							0.175				0.058			0.093	
Mg# (Fe <sub>T</sub> )							<b>75.9</b>				<b>89.4</b>			<b>83.3</b>	

<sup>a</sup> Mg/(Mg + Fe<sup>2+</sup> + Fe<sup>3+</sup>)<sup>b</sup> Bédard (1988).

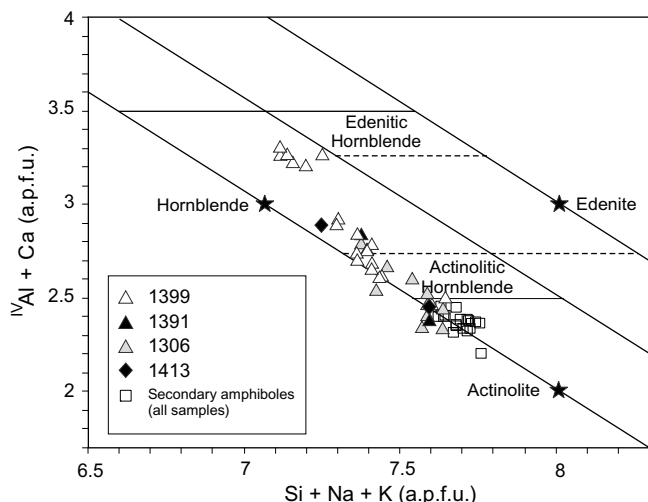


**Fig. 2.** Cationic diagram  $\text{Al}^{\text{IV}} + \text{Ca}$  vs.  $\text{Si} + \text{Na} + \text{K}$  showing a compositional trend of amphiboles from Sierra Norte spessartite lamprophyres. The black stars indicate the end-members compositions.

Potassium feldspars were identified in all samples but only are analyzed in 1391 groundmass and have a constant composition ( $\text{Or}_{96}$ ). Feldspar compositions are shown in Fig. 3.

#### 4.2. Whole-rock geochemistry

Results of whole-rock major and minor element analyses, REE analyses and normative compositions are presented in Table 2. The lamprophyres are chemically equivalent to subalkaline basalts in the TAS diagram (Fig. 4a). Analytical data were recalculated on a volatile-free basis and show low  $\text{SiO}_2$  contents (51.1–55.3 wt.%),  $\text{Al}_2\text{O}_3$  (12–16.6 wt.%),  $\text{CaO}$  (4.2–8.7 wt.%), and moderate total alkali contents (1.5–4.7 wt.%) are somewhat lower than those of andesites and basalts from orogenic regions (e.g., Suzuki and Shiraki, 1980; Wilson, 1989). They are calc-alkaline lamprophyres according to the classification scheme of Rock (1987) in a  $\text{K}_2\text{O}$  vs.  $\text{SiO}_2$  diagram (Fig. 4b). The dykes are over-saturated with respect to silica, containing both normative hypersthene and quartz. In terms of fer-

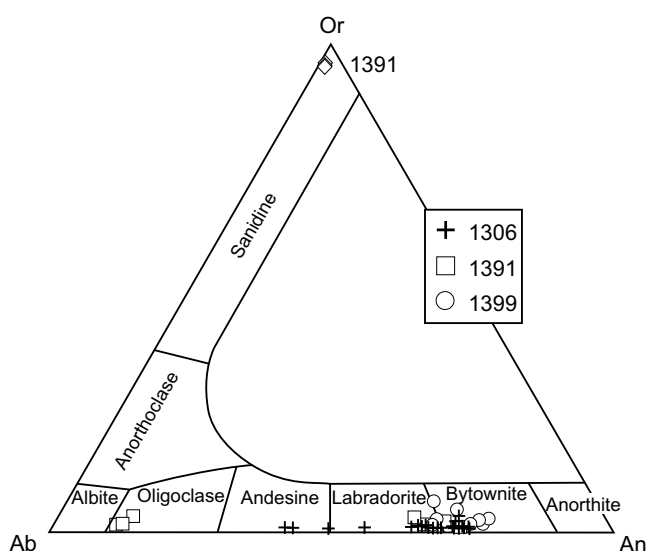


**Fig. 3.** Feldspars analyses of Sierra Norte spessartite lamprophyres plotted in the Or-Ab-An triangle of Deer et al. (1963).

**Table 2**

Major, minor, and trace elements concentrations and normative compositions of some spessartite lamprophyres from central Sierra Norte-Ambargasta

Sample wt.%	1306	1391	1395	1399	1413
$\text{SiO}_2$	51.10	52.90	54.30	53.50	55.32
$\text{TiO}_2$	1.02	0.66	0.79	0.59	0.81
$\text{Al}_2\text{O}_3$	15.50	13.20	14.90	12.50	16.97
$\text{Fe}_2\text{O}_3$	10.00	8.54	7.87	8.19	8.17
$\text{MgO}$	7.93	10.50	5.87	11.80	4.38
$\text{MnO}$	0.20	0.15	0.13	0.15	0.19
$\text{CaO}$	8.94	7.00	4.51	7.42	7.89
$\text{Na}_2\text{O}$	1.32	2.19	4.17	1.48	2.96
$\text{K}_2\text{O}$	1.70	1.39	0.92	0.91	1.29
$\text{P}_2\text{O}_5$	0.13	0.13	0.16	0.13	0.20
$\text{Cr}_2\text{O}_3$	0.06	0.17	0.03	0.19	n.d.
LOI	2.20	3.30	6.60	3.15	1.81
Total	100.10	100.13	100.25	100.01	99.99
Mg# <sup>a</sup>	65	74	63	77	55
ppm					
Rb	123	53	34	23	105
Sr	213	239	250	211	387
Ba	262	369	452	267	203
Y	21	19	18	17	21
Zr	110	109	126	113	134
Nb	4	6	8	6	11
Mo	<2	<2	s.d.	s.d.	<2
Ag	<0.5	<0.5	s.d.	s.d.	<0.5
In	<0.2	<0.2	s.d.	s.d.	<0.2
Sn	2	1	s.d.	s.d.	2
Sb	1.4	<0.5	s.d.	s.d.	2.3
Cs	11.3	6	s.d.	s.d.	14.9
Hf	3	2.9	s.d.	s.d.	4.1
Ta	0.2	0.4	s.d.	s.d.	0.3
W	3	20	s.d.	s.d.	2
Tl	1	0.5	s.d.	s.d.	0.8
Pb	<5	6	s.d.	s.d.	<5
Bi	<0.4	<0.4	s.d.	s.d.	<0.4
Th	1.8	4	s.d.	s.d.	4.1
U	0.4	0.9	s.d.	s.d.	1.4
V	213	166	s.d.	s.d.	179
Cr	335	988	139*	814*	27
Co	46	40	s.d.	s.d.	22
Ni	60	189	s.d.	s.d.	<20
Cu	134	49	s.d.	s.d.	<10
Zn	98	87	s.d.	s.d.	83
Ga	17	15	s.d.	s.d.	19
Ge	2	2	s.d.	s.d.	3
As	<5	<5	s.d.	s.d.	6
Sc	s.d.	33	s.d.	s.d.	25
Sample ppm	1306	1391	1413		
La	9.80	13.70	20.50		
Ce	20.40	27.90	42.20		
Pr	2.65	3.34	4.92		
Nd	11.90	13.80	19.90		
Sm	3.00	3.00	4.10		
Eu	1.18	0.88	1.46		
Gd	3.20	3.00	3.80		
Tb	0.60	0.50	0.60		
Dy	3.90	3.00	3.80		
Ho	0.80	0.60	0.70		
Er	2.40	1.80	2.20		
Tm	0.34	0.26	0.32		
Yb	2.20	1.70	2.20		
Lu	0.36	0.27	0.34		
REE total	62.73	73.75	107.04		
LREE	47.75	61.74	91.62		
HREE	13.80	11.13	13.96		
La/Lu	27.22	50.74	60.29		
CIPW normative compositions					
Sample	1306	1391	1395	1399a	1413
Q	9.06	7.26	9.60	10.96	12.35
or	10.28	8.51	5.81	5.57	7.77
ab	11.40	19.15	37.65	12.94	25.48
an	31.99	22.81	20.50	25.59	29.70
Di (wo)	5.25	5.15	1.01	4.89	3.75
Di (en)	4.53	4.44	0.87	4.22	3.23
Di (fs)	0.00	0.00	0.00	0.00	0.00
Hy (en)	15.73	22.71	14.81	26.30	7.92
Hy (fs)	0.00	0.00	0.00	0.00	0.00
mt	0.67	0.51	0.45	0.51	0.62
he	9.76	8.49	8.09	8.12	7.89
il	0.00	0.00	0.00	0.00	0.00
ap	0.29	0.29	0.37	0.29	0.44

\*0.899 =  $\text{FeO}$ .

<sup>a</sup>  $(\text{Mg}/(\text{Mg} + \text{Fe})) \times 100 - \text{Fe}_2\text{O}_3$ .

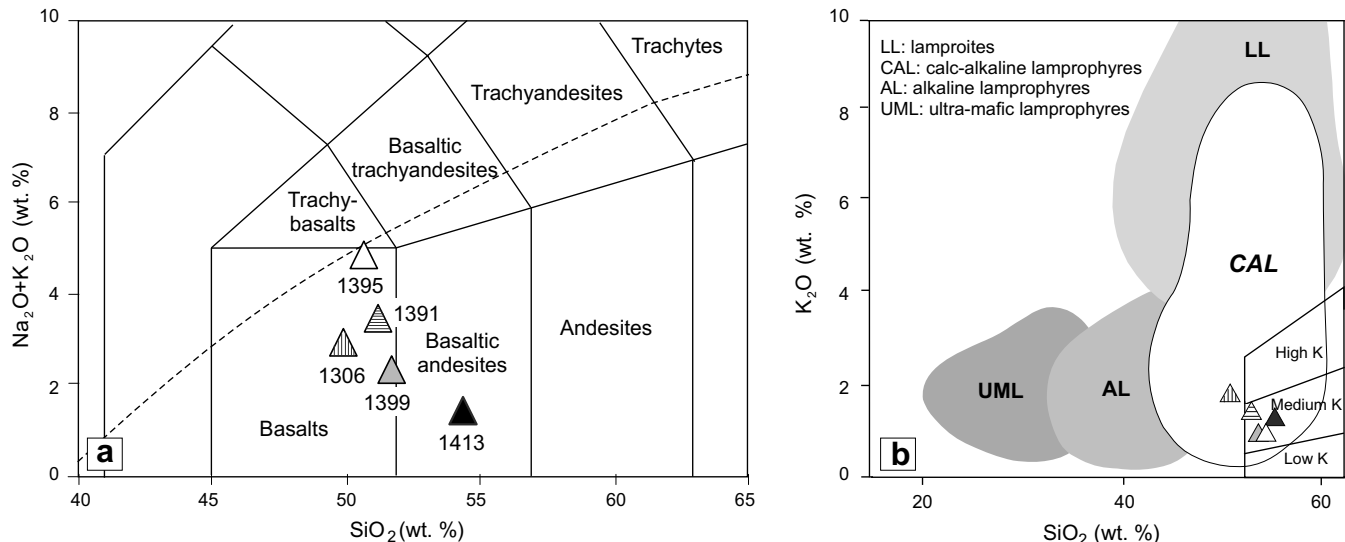


**Fig. 4.** Chemical classification of the lamprophyres. (a) TAS diagram (dates are re-calculated to a volatile-free basis). The line separates alkaline from subalkaline rocks (Irvine and Baragar, 1971). (b) Classificatory scheme of lamprophyres (Rock, 1987), samples as in Fig. 4a. The studied lamprophyres are typical medium-K calc-alkaline type.

romagnesian element abundances, the high Mg# (55–77), Cr (27–988 ppm) and Ni contents (60–190 ppm) indicate the relatively primitive nature of the dykes (Rock et al., 1988).

The lamprophyres show an enrichment of Rb (23–147 ppm), Ba (203–452 ppm), Sr (211–387 ppm) and other large ion lithophile elements (LILE) relative to HFSE (high field strength elements), especially Ta (0.2–1.6 ppm), Nb (4–11 ppm) and Y (17–21 ppm). MORB-normalized spidergrams (Fig. 5) show an irregular pattern, characterized by relative enrichments (15–120 times) of the

incompatible elements (Rb, K and Ba), with a strong positive spike in Rb and negative troughs in Nb, Ta, P and Ti, whereas Sr shows a rather uniform normalized concentration clustered around Sr<sub>N</sub> = 3. The Cs<sub>N</sub> is 850 to 2200 times higher than MORB. This pattern is similar to those of the average spessartite (Rock, 1991) and other calc-alkaline lamprophyres (e.g., Tate and Clarke, 1993; Hoch et al., 2001; Guo et al., 2004). In comparison, the studied spessartites patterns are slightly depleted in Sr, Th, Ta, Ce and P (HFSE and LREE) and present a positive spike in Rb. The Sierra Norte lam-

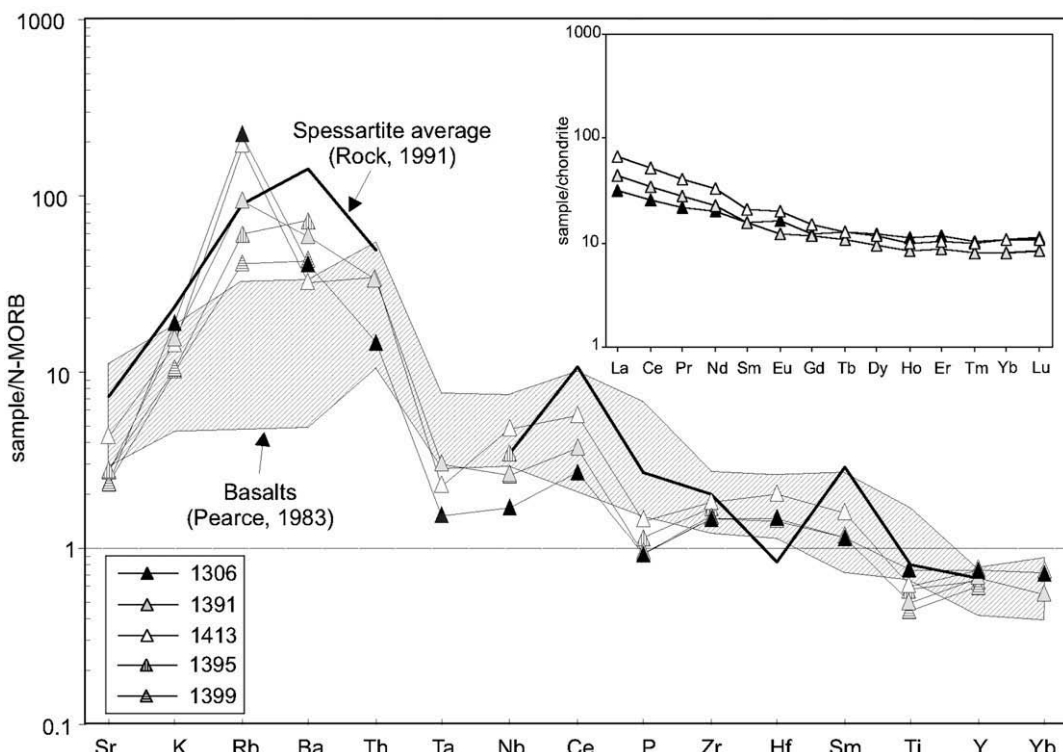


**Fig. 5.** MORB normalized multi-element diagram comparing the geochemical compositions of studied lamprophyres with average spessartite (Rock, 1991) and Phanerozoic continental margin basalts (Pearce, 1983). Normalization values after Sun and McDonough (1989). The inset shows the chondrite normalized REE diagram (normalization factors after Boynton, 1989). See text for further details.

**Table 3**

Sr, Nd, and Pb isotopic compositions of spessartite lamprophyres from central Sierra Norte-Ambargasta

Sample	Rb (ppm)	Sr (ppm)	$^{87}\text{Rb}/^{86}\text{Sr}$	Error	$^{87}\text{Sr}/^{86}\text{Sr}$	Error	$(^{87}\text{Sr}/^{86}\text{Sr})_0$	$\varepsilon_{\text{Sr}}(T)$	
1391	57.5	244.5	0.681	0.006	0.712047	0.000035	0.70738	49.18	
1399	31.6	220.2	0.416	0.014	0.708352	0.000081	0.70550	22.49	
1413	110.6	395.0	0.811	0.006	0.712947	0.000052	0.70738	49.26	
1306	136.5	224.8	1.760	0.026	0.719504	0.000061	0.70743	49.94	
Sm (ppm)	Nd (ppm)	$^{147}\text{Sm}/^{144}\text{Nd}$	Error	$^{143}\text{Nd}/^{144}\text{Nd}$	Error	$(^{143}\text{Nd}/^{144}\text{Nd})_0$	$\varepsilon_{\text{Nd}}(T)$	$T_{\text{DM}}$ (Ga)	
1391	3.183	13.964	0.1378	0.0005	0.512211	0.000009	0.511773	-4.31	1.7
1399	3.114	13.766	0.1368	0.0005	0.512241	0.000008	0.511806	-3.66	1.6
1413	4.275	19.821	0.1304	0.0004	0.512196	0.000008	0.511782	-4.14	1.5
1306	3.123	12.002	0.1573	0.0005	0.512435	0.000012	0.511935	-1.14	1.6
		$^{206}\text{Pb}/^{204}\text{Pb}$	Error ( $2\sigma$ )	$^{207}\text{Pb}/^{204}\text{Pb}$	Error ( $2\sigma$ )	$^{208}\text{Pb}/^{204}\text{Pb}$	Error ( $2\sigma$ )		
1391	19.014		0.009	15.671		39.173		0.013	
1399	19.207		0.005	15.701		39.477		0.005	
1413	20.137		0.015	15.759		39.908		0.015	
1306	18.749		0.012	15.692		38.860		0.013	

lamprophyres seem to be broadly similar in chemical composition to modern and Phanerozoic continental margin basalts (Pearce, 1983); Fig. 5 shows a similar pattern with an average composition of basalts except for a larger enrichment of K and Rb.

The transition elements (V, Cr, Co and Ni) show different behaviors according to the degree of differentiation; the most primitive samples have compositions close to those of MORB, particularly the sample 1391 which has high Cr abundances (988 ppm), whereas the most differentiated sample (1413) is depleted in the same elements respect to MORB.

Chondrite normalized data (Fig. 5) exhibit fractionated REE distribution patterns (Boynton, 1989) with enrichment for LREE (30–70 times), and a flat pattern of HREE (<10 times chondrite). Samples 1306 and 1413 show a slightly positive Eu anomaly and sample 1391 shows a smooth negative Eu anomaly ( $\text{Eu}/\text{Eu}' = 0.9$ ). The more primitive Sierra Norte lamprophyres are depleted in REE respect to other lamprophyric suites (e.g., Tate and Clarke, 1993; Hoch et al., 2001; Guo et al., 2004), except for sample 1413, which represents the most geochemically evolved lamprophyre of the studied samples.

#### 4.3. Sr, Nd, and Pb isotopes

Sr, Nd, and Pb isotope compositions were studied to provide further constraints on the source and crustal interaction during magma evolution. The analytical results are listed in Table 3.

The present-day ratios of  $^{87}\text{Sr}/^{86}\text{Sr}$  from Sierra Norte lamprophyres range from 0.70835 to 0.71950, and  $^{143}\text{Nd}/^{144}\text{Nd}$  range from 0.51219 to 0.51243. Within the Rb-Sr isochronic diagram three analytical points (whole-rock samples 1391, 1306 and 1413) defined a line with a slope that corresponds to an age of  $485 \pm 25$  Ma, with an initial strontium ratio of  $0.706 \pm 0.016$  (Fig. 6). The ( $\text{epsilon}$ ) $\varepsilon_{\text{Sr}}$  at 485 Ma ranges from 49.9 to 22.5, and individual ( $^{87}\text{Sr}/^{86}\text{Sr}$ ) $_i$  values are between 0.70743 and 0.7055. All lamprophyres have negative ( $\text{epsilon}$ ) $\varepsilon_{\text{Nd}}$  values calculated for 485 Ma, ranging from -4.31 to -1.14, with a relatively constant  $^{143}\text{Nd}/^{144}\text{Nd}$ , between 0.51193 and 0.51177. In the ( $^{87}\text{Sr}/^{86}\text{Sr}$ ) $_i$  vs. ( $\text{epsilon}$ ) $\varepsilon_{\text{Nd}}(485 \text{ Ma})$  diagram (Fig. 7) the samples plot between EM I and EM II (enriched mantle type I and II). In comparison, these spessartites are less radiogenic than calc-alkaline lamprophyres of other localities (e.g., minettes, Hoch et al., 2001) but Late Carboniferous lamprophyres from Europe show similar isotope compositions. The European lamprophyres (minettes and kersantites) are interpreted as melts of a mantle source that was enriched due to the recycling of continental crust at an active margin (Hegner et al., 1998; Turpin et al., 1988). The Pb isotope compositions are  $^{208}\text{Pb}/^{204}\text{Pb}$  (38.8–39.9),  $^{207}\text{Pb}/^{204}\text{Pb}$  (~15.7), and  $^{206}\text{Pb}/^{204}\text{Pb}$

(18.7–20.1). In the  $^{208}\text{Pb}/^{204}\text{Pb}$  and  $^{207}\text{Pb}/^{204}\text{Pb}$  vs.  $^{206}\text{Pb}/^{204}\text{Pb}$  diagrams the samples plot close the upper crust curve of the plumbosilicate mineralization (Fig. 5).

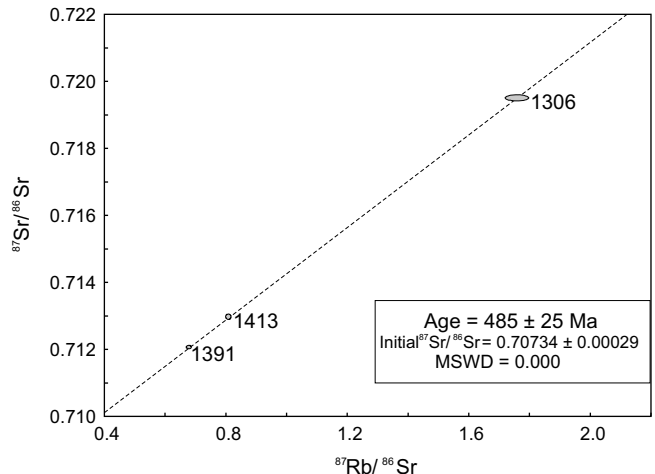


**Fig. 6.** Whole rock Rb-Sr isochron of Sierra Norte-Ambargasta spessartite lamprophyres. (Data-point error ellipses are 68.3% conf.). Samples plotted are 1391, 1413 and 1306.

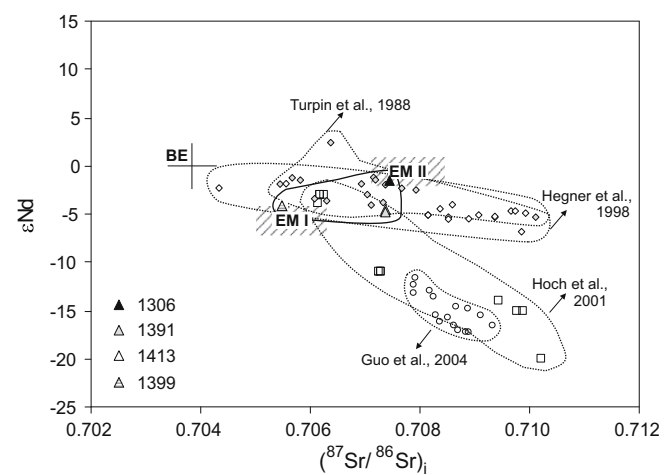


**Fig. 7.** ( $^{87}\text{Sr}/^{86}\text{Sr}$ ) $_i$  vs.  $\varepsilon_{\text{Nd}}$  diagram. The contoured fields contain published data of calc-alkaline lamprophyres from other localities. BE: bulk earth. EM I and II: enriched mantle type I and II (Zindler and Hart, 1986). See text for further details.

tectonic model of Zartman and Doenot shown (1981), and fall near the mantle Northern Hemisphere Reference Line of Hart (1984), close to lamprophyric rocks of other localities (Fig. 8).

The Sm–Nd depleted-mantle model ages (DePaolo, 1981) are around 1.7 Ga, what suggest the age of the mantle metasomatism event associated with magmatic arc evolution during the Pampean orogeny.

In summary, the available isotopic information of studied lamprophyres indicate enriched mantle-derived magmas as the main magma's source, although some crustal contamination during the magma ascent to the upper crustal levels can not be rejected.

## 5. Discussion

### 5.1. Petrogenesis

The Sierra Norte lamprophyres can be classified as spessartites; considering the phenocrysts mineralogy, they were recognized as augite spessartites and hornblende spessartites. Petrographical, mineralogical, geochemical and isotopic features of dykes indicate a common genetic relationship and allow us to propose a similar origin and a common parental magma.

The presence of minerals with elongate habit and porphyritic textures suggests rapid crystallization and cooling during the emplacement. Xenocrystic quartz and feldspars occur in some samples, suggesting partial crustal contamination by assimilation of country rock. Clinopyroxenes composition suggests a high crystallization pressure and is compatible with the presence of associated hornblende.

Suzuki and Shiraki (1980) discussed the stability range of the hornblende–clinopyroxene assemblage in experimental studies of water-saturated systems ( $\text{SiO}_2 = 50\text{--}60\text{ wt.\%}$ ), concluding, with reference to crystallization pressure, that: (a) the phenocrystic hornblendes in hornblende–spessartites might have crystallized on the liquidus from a magma of andesitic composition at pressures greater than 8 Kbar under water-saturated conditions, and (b) the groundmass hornblendes and the fine-grained spessartites might have crystallized under pressures between 4 and 1 kbar.

The similarities of the whole-rock  $\text{SiO}_2$  content and the composition of the phenocrysts of the early mafic assemblage of the studied Sierra Norte lamprophyres, with the experimental data of Suzuki and Shiraki (1980), might suggest that mafic phenocrystic phases crystallized under initial pressures that were much higher than final emplacement pressures. This fact would also imply fast

ascent and cooling to prevent mafic phenocrysts from re-equilibration.

The emplacement pressure for the lamprophyres is estimated to be less than 3 kbar; this estimation is based on the fact that lamprophyric dikes crosscut brittle dacite–rhyolite rocks of the subvolcanic CDLB body and of the granodiorite–monzogranite country rocks of the GM suite, which, according to Poklepovic et al. (2005) were emplaced at maximum pressures of  $2.5 \pm 0.5$  kbar and  $3 \pm 0.6$  kbar, respectively.

The slight compositional variation of hornblende in all lamprophyres, the absence of hornblende zonation, the Mg# in agreement with Bédard's Mg# value, and its chemical composition indicate a primary origin for these amphiboles (Pe-Piper, 1988). The principal substitutions registered in lamprophyric hornblendes suggest crystallization from a mafic to intermediate silica-saturated to oversaturated alkaline magma.

Experimental evidence in basalts indicate that the stability field of plagioclase is reduced by increasing water pressure (Bédard, 1988); some previous contributions (e.g. Lange et al., 1993; Carmichael et al., 1996) consider that in magmas with  $\text{SiO}_2$  concentrations close to 60 wt.\%, the abundance of primary amphibole and the nearly absent phenocrystic plagioclase could be evidence of melts with high water contents. In the same direction, experimental work that aimed to reproduce hornblende phenocrysts without coexisting plagioclase or pyroxene phenocrysts in spessartites, needed water saturation at  $\sim 3$  kbar, corresponding to  $>5.5\%$  water in the melt (Moore and Carmichael, 1998). At lower pressures and concentrations of water, hornblende was replaced by orthopyroxene, augite and plagioclase (Carmichael et al., 1996).

### 5.2. Magma source

Most of the dykes are representative of primitive compositions, with high Mg# and Ni and Cr contents close to MORB, and show high concentrations of transition elements. In some cases (samples 1306 and 1413), the slightly positive Eu anomaly restricts the lamprophyric magma formation to a free-plagioclase source, (e.g. peridotite or pyroxenite), and in others (sample 1391), the smooth negative Eu anomaly ( $\text{Eu}/\text{Eu}^* = 0.9$ ) can be explained by minor plagioclase fractionation. The HREE contents,  $<10$  times chondrite, are compatible with retention of these elements in the residual magma as a result of fractionation of garnet in the source, and the HFSE content range is similar to that of a depleted mantle. The LILE abundance (15–220 times MORB) and the LREE (30–70 times chon-

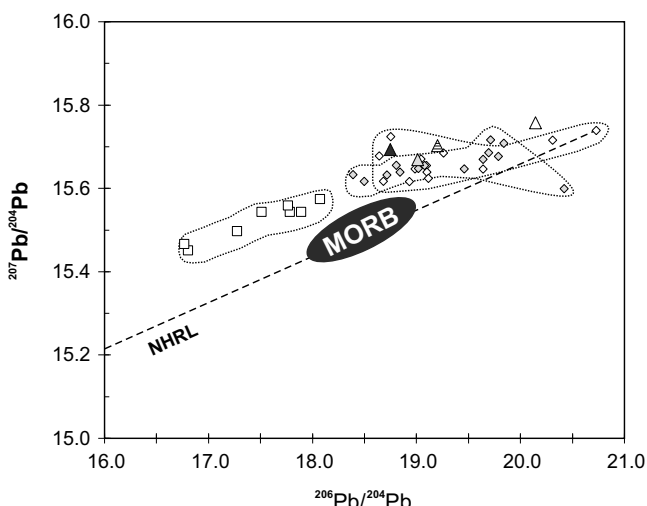
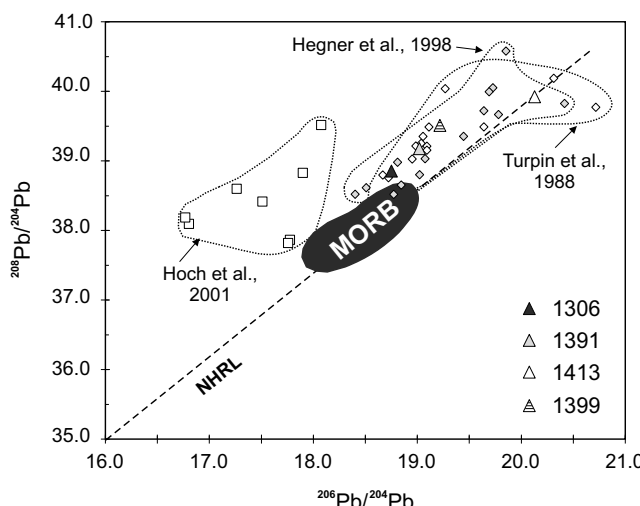


**Fig. 8.** Pb isotope diagrams of Sierra Norte spessartite lamprophyres compared with MORB and lamprophyres from other localities. See text for further details.

drite) suggest an incompatible elements enriched source. The Ba/La (9–27), Pb/La (0.4–1.9) and Cs/Rb (0.09–0.15) ratios are very high compared to MORB values (3–10, 0.09–0.12 and 0.013, respectively), which suggest an important contribution from sediments to magma, also consistent with the Ce positive anomaly ( $Ce/Ce^* = 2.15\text{--}2.63$ ). The  $(^{87}\text{Sr}/^{86}\text{Sr})_{\text{i}}$ ,  $(\text{epsilon})_{\text{Nd}}$ , and high  $^{207}\text{Pb}/^{204}\text{Pb}$  and high  $^{206}\text{Pb}/^{204}\text{Pb}$  values indicate a mantle-derived magma with an important crustal contamination. The origin of a crustal component in lamprophyric magmas has been studied by many authors (e.g., Turpin et al., 1988; Carmichael et al., 1996; Hoch et al., 2001), from whom two classical interpretations arise: (a) contamination of mantle-derived magma during emplacement, and (b) formation of an enriched lithospheric mantle reservoir during a subduction process. Our data is insufficient to be able to favor one interpretation over the other.

Several authors (e.g. MacDonald et al., 1985; Barnes et al., 1986) propose a multiple origin source hypotheses for some calc-alkaline lamprophyres, resulting from a contribution of sub-continental lithospheric mantle (LILE high contents and HFSE variably high) and asthenospheric mantle (HFSE, Cr and Ni high contents) with a metasomatic component derived from subducted pelagic sediments (low Nb contents and high volatiles) and variably contaminated by a crustal component. The Sierra Norte lamprophyres show a geochemical and isotopic signature compatible with those characteristics, indicating similar sources.

### 5.3. Tectonic setting and emplacement age

The calc-alkaline lamprophyres are, in essence, products of subduction-related magmatism (Rock, 1991). They are usually emplaced at convergent margins as dykes that intruded calc-alkaline granitic rocks. Several authors related lamprophyres to continental collision events, whereas others indicated its relation with arc setting; in both, the cortical material, crust or sediments, are recycled into the mantle (Hoch et al., 2001). Using some immobile elements (Ta/Yb vs. Th/Yb diagram, Pearce, 1983, not shown) the studied rocks of Sierra Norte suggest an active continental margin setting, and derivation from an enriched mantle metasomatized during the subduction of oceanic lithosphere. Other evidence for this source is the Zr and Y contents (109–120 ppm and 17–25 ppm, respectively) which relate the Sierra Norte lamprophyres with active continental margin magmas (Pearce, 1983). Likewise, the high Ba/Ti values are typical of subduction zone magmas. The ages of lamprophyres (see below) and their geologic setting within the Sierra Norte magmatic arc relate their intrusion to the terminal stage of subduction.

The isotopic features indicate a possible derivation from an enriched subcontinental mantle source, modified by a subduction event, and petrography suggests that this magma was contaminated with upper continental crust during ascent and/or emplacement. This geological setting was previously proposed as the origin of the Sierra Norte-Ambargasta batholith (Ramos, 1988; Kraemer et al., 1995; Lira et al., 1997; Rapela et al., 1998), indicating the emplacement of a magmatic arc in the protomargin of Gondwana as a consequence of the approach of the Pampia terrane to Córdoba basement, with the main magmatic activity taking place during the Late Proterozoic to the Late Cambrian (Leal et al., 2003; Millone et al., 2003). Recently, another scenario was proposed (Gromet et al., 2005, and references therein) who suggest a ridge subduction process without the existence of a continental collision as origin for the Sierra Norte-Ambargasta batholith.

The isotopic signature of the lamprophyres is compatible with a post-collisional emplacement during the Ordovician times, and the  $T_{\text{DM}}$  (1.7 Ga) suggests the involvement of a crust with affinities with a basement located to the west of a remarkable tectonic boundary existent between the Río de la Plata craton and the Pampean Ranges in agreement with the most recent publications (Leal

et al., 2003; Rapela et al., 2005; Gromet et al., 2005). The age of the lamprophyres ( $485 \pm 25$  Ma) is virtually identical to the emplacement ages of other small bodies and dykes from the Oncán rhyolite unity (Rapela et al., 1991; Correa, 2003; Millone, 2004; O'Leary et al., 2006) and is comparable with the age of a hydrothermal event registered in the Cerro de los Burros dacite–rhyolite subvolcanic body (Leal et al., 2003). All these ages support the existence of a regional post-collisional event during the Early Ordovician, ca. 490 Ma.

## 6. Conclusions

Calc-alkaline lamprophyre dykes emplaced in the Sierra Norte-Ambargasta batholith during Early Ordovician times are spessartites; their main mineralogy is represented by magnesiohornblende  $\pm$  augite and calcic plagioclase, which is product of primary magmatic crystallization. The Sierra Norte lamprophyric suite geochemically resembles basalts and low silica andesites, with  $\text{SiO}_2$  contents ranging from 51.1 to 55.3 wt.%, moderate  $\text{Na}_2\text{O} + \text{K}_2\text{O}$  contents from 1.5 to 4.7 wt.%, and high volatile contents (LOI values ranging from 1.8 to 6.6). The lamprophyres have Mg# between 55 and 77, and high Cr contents (27–988 ppm).

The calc-alkaline nature of Sierra Norte lamprophyres is depicted in the MORB-normalized patterns, which show an enrichment in LILE relative to HFSE, and a negative Nb-Ta anomaly that is typical of calc-alkaline lamprophyres characteristic of destructive plate-margin magmatism; this has been interpreted as indicative of assimilation of subducted sediment. Chondrite-normalized REE patterns are fractionated with  $\text{Ce}_{\text{N}} = 25\text{--}52$  and  $\text{Yb}_{\text{N}} = 8.1\text{--}10.5$ . The lamprophyres show a limited range in initial  $(^{87}\text{Sr}/^{86}\text{Sr})_{\text{i}}$  (0.705–0.707),  $(\text{epsilon})_{\text{Nd}(T)}$  (−1.45 to −4.57), and have high  $^{207}\text{Pb}/^{204}\text{Pb}$  and high  $^{206}\text{Pb}/^{204}\text{Pb}$  values. The isotopic features indicate a possible derivation from an enriched subcontinental mantle source, modified by a subduction event, with subordinated contributions of upper crust material to lamprophyric magma. The  $T_{\text{DM}}$  (1.7 Ga) suggests a crustal component with affinities to the basement of the Pampean Ranges.

The mineralogical, geochemical and isotopic information indicates a source related to a subduction setting and suggest the emplacement of the Sierra Norte lamprophyric suite at the final stage of the Pampean orogeny, in a regional extensional setting developed in the Sierra Norte-Ambargasta batholith during a post-collisional event in the Early Ordovician.

## Acknowledgements

We are indebted to the financial support provided by the Agencia Nacional de Promoción Científica y Tecnológica (ANPCYT, projects PICT 07-03581 and PICT-R No. 179). M.S.O. is grateful to J. Silvestro for informal manuscript reviews, to the Consejo Nacional de Investigaciones Científicas y Técnicas (CONICET, Argentina) for a doctoral fellowship, and to the Conselho Nacional de Desenvolvimento Científico e Tecnológico (CNPq, Brazil) for a post-doctoral research stay. We thank H.A. Millone for fieldwork and sample preparation assistance. The manuscript greatly benefited from reviews by M. López de Lucchi and E. Gregori.

## References

- Baldo, E.G., Pankhurst, R.J., Rapela, C.W., Saavedra, J., Mazzieri, C., 1998. Granito "El Cerro", magmatismo colisional famatiniano en el sector austral de la Sierra Norte-Ambargasta, Córdoba. X Congreso Geológico Argentino y VI Congreso Nacional de Geología Económica 2, 374–378.
- Barnes, R.P., Rock, N.M.S., Gaskarth, J.W., 1986. Late Caledonian dyke-swarms in Southern Scotland: new field, petrological and geochemical data for the Wigtown Peninsula, Galloway. Geological Journal 21, 101–125.

- Bédard, J.H., 1988. Comparative amphibole chemistry of the Monteregeian and White Mountain alkaline suites, and the origin of amphiboles megacrysts in alkali basalts and lamprophyres. *Mineralogical Magazine* 52, 91–103.
- Bédard, J.H., Francis, M.D., Ludden, J., 1988. Petrology and pyroxene chemistry of Monteregeian dykes: the origin of concentric zoning and green cores in clinopyroxenes of alkali basalts and lamprophyres. *Canadian Journal of Earth Sciences* 25, 2041–2058.
- Boynton, N.V., 1989. Cosmochemistry of the rare earth elements: condensation and evaporation processes. In: Lipin, B.R., McKay, G.A. (Eds.), *Geochemistry and Mineralogy of Rare Earth Elements*. Mineralogy Society of America, *Reviews in Mineralogy* 21, pp. 1–24.
- Carmichael, I.S.E., Lange, R.A., Luhr, J.F., 1996. Quaternary minettes and associated volcanic rocks of Mascota, western Mexico: a consequence of plate extension above a subduction modified mantle wedge. *Contributions to Mineralogy and Petrology* 124, 302–333.
- Correa, M.J., 2003. Petrología y edad K/Ar de diques relacionados a la Formación Oncán, sierra de Ambargasta, Santiago del Estero. *Revista de la Asociación Geológica Argentina* 58 (4), 664–668.
- Daziano, C.O., 1986. El magmatismo básico en el batolito de Achala. Estudio geológico-petrográfico de los filones lamprofíricos del flanco oriental y los basaltos olivínicos del borde centro-occidental, Sierra Grande de Córdoba. *Boletín de la Asociación Geológica de Córdoba* 8, 551–555.
- Deer, W.A., Howie, R.A., Zussman, J., 1963. Rock-forming minerals. Framework Silicates, vol. 4. Longmans/Green and Co. Ltd., London, p. 435.
- DePaolo, D.J., 1981. A neodymium and strontium isotopic study of the Mesozoic calc-alkaline granite batholiths of the Sierra Nevada and Peninsular Ranges, California. *Journal of Geophysical Research* 86 (B11), 10470–10488.
- Dorais, M.J., 1990. Compositional variations in pyroxenes and amphiboles of the Belknap Mountain complex, New Hampshire: evidence for the origin of silica-saturated alkaline rocks. *American Mineralogist* 75, 1092–1105.
- Franchini, M., Lira, R., Meinert, L., Ríos, J., Poklepovic, M.F., Impiccini, A., Millone, H.A., 2005. Na–Fe–Ca alteration and LREE (Th–Nb) mineralization in marble and granitoids of Sierra de Sumampa, Santiago del Estero, Argentina. *Economic Geology* 100 (4), 733–764.
- Gordillo, C.E., 1955. Estudio Químico-Petrográfico del Cerro "El Périgón" y las rocas magnéticas vecinas-Sierra Norte de Córdoba (Argentina). *Revista de la Facultad de Ciencias Exactas, Físicas y Naturales, Universidad Nacional de Córdoba*, Año 17 (3–4), 755–780.
- Sanchez Granel, J.I., Prieto Zehndel, A.E., Andrade, M.Y., 1967. Estudio sobre supuestos lamprófiros de la Sierra Norte de Córdoba. Seminario II, Facultad de Ciencias Exactas, Físicas y Naturales, Universidad Nacional de Córdoba (unpublished).
- Gromet, L.P., Otamendi, J.E., Miró, R.C., Demichelis, A.H., Schwartz, J.J., Tibaldi, A.M., 2005. The Pampean orogeny: ridge subduction or continental collision? *Gondwana* 12, Academia Nacional de Ciencias, Mendoza, Argentina, Abstract 183.
- Guo, F., Fan, W., Wang, Y., Zhang, M., 2004. Origin of early cretaceous calc-alkaline lamprophyres from the Sulu orogen in eastern China: implications for enrichment processes beneath a continental collision belt. *Lithos* 78, 291–305.
- Hart, S.R., 1984. A large-scale isotope anomaly in the southern hemisphere mantle. *Nature* 309, 753–757.
- Hegner, E., Kölbl-Ebert, M., Loeschke, J., 1998. Post-collisional Variscan lamprophyres (Black Forest, Germany):  $^{40}\text{Ar}/^{39}\text{Ar}$  phlogopite dating, Nd, Pb, Sr isotope, and trace element characteristics. *Lithos* 45, 395–411.
- Hoch, M., Rehkämper, M., Tobschall, H.J., 2001. Sr, Nd, Pb, and O isotopes of minettes from Schirmacher Oasis, East Antarctica: a case of mantle metasomatism involving subducted continental material. *Journal of Petrology* 42, 1387–1400.
- Irvine, T.N., Baragar, W.R.A., 1971. A guide to the chemical classification of the common volcanic rocks. *Canadian Journal of Earth Sciences* 8, 523–548.
- Kawashita, K., 1972. O método Rb–Sr em rochas sedimentares. Aplicação para as Bacias do Paraná e Amazonas. Tese de doutorado (unpublished), Instituto de Geociências, Universidade de São Paulo, p. 111.
- Koukharsky, M., Munizaga, F., Leal, P., Correa, M.J., Brodtkorb, M.K. de, 1999. New K/Ar ages in the Ambargasta and Norte de Córdoba Ranges, Argentina. In: II Simposio Sudamericano de Geología Isotópica, Villa Carlos Paz, Córdoba, Argentina. Instituto de Geología y Recursos Minerales, Servicio Geológico Minero Argentino, Anales 34, pp. 76–77.
- Kraemer, P.E., Escayola, M.P., Martino, R.D., 1995. Hipótesis sobre la evolución tectónica neoproterozoica de las Sierras Pampeanas de Córdoba (30°40'–32°40'). *Revista de la Asociación Geológica Argentina* 50, 47–59.
- Lange, R.A., Carmichael, I.S.E., Renne, P.R., 1993. Potassic volcanism near Mono basin, California: evidence for high water and oxygen fugacities inherited from subduction. *Geology* 21, 949–952.
- Leake, B.E., Wooley, A.R., Arps, C.E.S., Birch, W.D., Gilbert, M.C., Grice, J.D., Hawthorne, F.C., Kato, A., Kisch, H.J., Krivovichev, V.G., Linthout, K., Laird, J., Mandarino, J.A., Maresch, W.V., Nickel, E.H., Rock, N.M.S., Schumacher, J.C., Smith, D.C., Stephenson, N.C.N., Ungaretti, L., Whittaker, E.J.W., Youzhi, G., 1997. Nomenclature of amphiboles: report of the subcommittee on amphiboles of the international mineralogical association, commission on new minerals and mineral names. *American Mineralogist* 82, 1019–1037.
- Leal, P.R., Hartmann, L.A., Santos, J.O.S., Ramos, V.A., Miró, R.C., 2003. Volcanismo postorogénico en el extremo norte de las sierras pampeanas orientales: nuevos datos geocronológicos y sus implicancias tectónicas. *Revista de la Asociación Geológica Argentina* 58 (4), 593–607.
- Lira, R., Millone, H.A., Kirschbaum, A.M., Moreno, R.S., 1997. Calc-alkaline arc granitoid activity in the Sierra Norte-Ambargasta Ranges, Central Argentina. *Journal of South American Earth Sciences* 10 (2), 157–177.
- López de Luchi, M.G., 1998. Petrología de diques lamprofíricos del noreste de la Sierra de San Luis. 10º Congreso Latinoamericano de Geología and 6º Congreso Nacional de Geología Económica, Actas II, p. 344.
- Lucero, H.N., 1948. Observaciones geológicas y petrográficas en la sección meridional de la Sierra Norte de Córdoba (entre Deán Funes y Quilino), con especial atención a los pórfitos cuarcíferos. Tesis Doctoral (unpublished), Universidad Nacional de Córdoba.
- Lucero, H.N., 1969. Descripción de las hojas geológicas 16h, Pozo Grande y 17h, Chuña Huasi, Provincias de Córdoba y Santiago del Estero. Dirección Nacional de Geología y Minería, Buenos Aires, Boletín 107, p. 39.
- Lucero Michaut, H.N., Gamkösán, A., Jarsún, B., Zamora, E., Sigismundi, M., Miró, R., Caminos, R., 1995. Mapa geológico de la provincia de Córdoba. República Argentina. Escala 1:500.000. Secretaría de Minería. Dirección Nacional del Servicio Geológico, Buenos Aires.
- Ludwig, K.R., 1999. Isoplots/Ex. Berkeley Geochronological Center. Special Publication 1, p. 41.
- MacDonald, R., Thorpe, R.S., Gaskarth, J.W., Grindrod, A.R., 1985. Multi-component origin of caledonian lamprophyres of northern England. *Mineralogical Magazine* 49, 485–494.
- Millone, H.A., 2004. Geoquímica y metalogénesis de sistemas hidrotermales con metales base, plata y oro en el basamento neoproterozoico de la Sierra Norte de Córdoba, Argentina. Tesis Doctoral (unpublished), Facultad de Ciencias Exactas, Físicas y Naturales, Universidad Nacional de Córdoba, p. 519.
- Millone, H.A., Tassinari, C.C.G., Lira, R., Poklepovic, M.F., 2003. Age and strontium-neodymium isotope geochemistry of granitoids of the Sierra Norte-Ambargasta batholith, central Argentina. IV South American Symposium on Isotope Geology, Salvador, Bahía, Brasil, Short papers, volume II, pp. 617–620.
- Minera TEA, 1968. Geología y Recursos Minerales de las Sierras de Ambargasta y Sumampa. Evaluación de los yacimientos manganíferos y posibilidades de beneficio mineral. Departamento de Ojo de Agua y Quebrachos. Provincia de Santiago del Estero vol. 1, p. 155 (unpublished).
- Miró, R.C., 2001. Hoja Geológica Villa Ojo de Agua, 1:250.000, Santiago del Estero y Córdoba. Instituto de Geología y Recursos Minerales, Servicio Geológico Minero Argentino.
- Miró, R.C., Schwartz, J., Gromet, P., 2005. Magmatismo calcoalcalino en la Sierra Norte de Córdoba. Su extensión temporal. In: Aceñolaza, F.G., Aceñolaza, G.F., Hünicken, M., Toselli, A.J. (Eds.), Simposio Bodenbender, INSUGEO, Serie Correlación Geológica 19, pp. 199–210.
- Moore, G., Carmichael, I.S.E., 1998. The hydrous phase equilibria (to 3 kbar) of an andesite and basaltic andesite from western Mexico: constraints on water content and conditions of phenocryst growth. *Contributions to Mineralogy and Petrology* 130, 304–319.
- Morimoto, N., Fabries, J., Ferguson, A.K., Ginzburg, I.V., Ross, M., Seifert, F.A., Zussman, J., Aoki, K., Gottardi, G., 1988. Nomenclature of pyroxenes. *American Mineralogist* 73, 1123–1133.
- O'Leary, M.S., 2004. Petrología, geoquímica y metalogénesis de los diques dacítico-riolíticos del arco magmático cambro-orodvílico de la Sierra Norte-Ambargasta, provincias de Córdoba y Santiago del Estero, República Argentina. Tesis Doctoral (unpublished), Facultad de Ciencias Exactas, Físicas y Naturales, Universidad Nacional de Córdoba, p. 337.
- O'Leary, M.S., Tassinari, C.C.G., Lira, R., 2006. Sr, Pb, and Nd isotopic signature of calc-alkaline porphyry dykes from the Sierra Norte-Ambargasta batholith, Eastern Sierras Pampeanas, Argentina. V South American Symposium on Isotope Geology, Punta del Este, Uruguay, Short papers, pp. 408–411.
- Orozco, B., Ortiz Suárez, A., 2005. Los lamprófiros de la Sierra de San Luis. 16º Congreso Geológico Argentino, La Plata. Actas I, 585–590.
- Pearce, J.A., 1983. Role of the sub-continental lithosphere in magma genesis at active continental margins. In: Hawkesworth, C.J., Norry, M.J. (Eds.), Continental Basalts and Mantle Xenoliths. Shiva Publishing Ltd., Nantwich, UK, pp. 230–249.
- Pe-Piper, G., 1988. Calcic amphiboles of mafic rocks of the Jeffers Brook plutonic complex, Nova Scotia, Canada. *American Mineralogist* 73, 993–1006.
- Poklepovic, M.F., Lira, R., Dorais, M.J., Millone, H.A., 2005. Consideraciones geobarométricas de los granitoides calco-alcalinos del batolito de Sierra Norte-Ambargasta, Córdoba, Argentina. 16º Congreso Geológico Argentino, La Plata. Actas I, 619–626.
- Pouchou, J.L., Pichoir, F., 1985. PAP (phi-ro-z) procedure for improved quantitative microanalysis. In: Armstrong, J.T. (Ed.), Microbeam Analysis. San Francisco Press, San Francisco, pp. 404–106.
- Ramos, V.A., 1988. Late proterozoic-early paleozoic of South America: a collisional story. *Episodes* 11, 168–174.
- Rapela, C.W., Pankhurst, R.J., Bonalumi, A.A., 1991. Edad y geoquímica del pórfito granítico de Oncán, Sierra Norte de Córdoba, Sierras Pampeanas, Argentina. 6º Congreso Geológico Chileno, 19–22.
- Rapela, C.W., Pankhurst, R., Casquet, C., Baldo, E., Saavedra, J., Galindo, C., Fanning, C.M., 1998. The Pampean orogeny of the southern proto-andes: Cambrian continental collision in the Sierras de Córdoba. In: Pankhurst, R., Rapela, C.W. (Eds.), The Proto-Andean Margin of Gondwana. Geological Society, London, Special Publication 142, pp. 181–217.
- Rapela, C.W., Fanning, C.M., Pankhurst, R.J., 2005. The Río de la Plata Craton: the search for its full extent. *Gondwana* 12, Academia Nacional de Ciencias, Mendoza, Argentina, Abstract 304.

- Rock, N.M.S., 1984. Nature and origin of calc-alkaline lamprophyres: minettes, vogesites, kersantites and spessartites. Royal Society of Edinburgh Transactions of Earth Sciences 74, 193–227.
- Rock, N.M.S., 1987. The nature and origin of lamprophyres: an overview. In: Fitton, J.G., Upton, B.G.J. (Eds.), Alkaline igneous rocks. Geological Society Special Publications 30, pp. 191–226.
- Rock, N.M.S., 1991. Lamprophyres. Blackie and Son Ltd., Glasgow. p. 285.
- Rock, N.M.S., Gaskart, J.W., Henney, P.J., Shand, P., 1988. Late Caledonian dyke swarms of Northern Britain: some preliminary petrogenetic and tectonic implications on their province-wide distribution and chemical variation. Canadian Mineralogist 26, 3–22.
- Sato, K., Tassinari, C.C.G., Kawashita, K., Petronilho, L., 1995. O método geocronológico Sm-Nd no IGC – USP e suas aplicações. Anais da Academia Brasileira de Ciências 67 (3), 313–336.
- Sims, J., Ireland, T., Camacho, A., Lyons, P., Pieters, P.E., Skirrow, R., Stuart-Smith, P.G., Miró, R., 1998. U-Pb, Th-Pb, and Ar-Ar geochronology from the Southern Sierras Pampeanas, Argentina: implications for the Paleozoic tectonic evolution of the western Gondwana margin. In: Pankhurst, R., Rapela, C.W. (Eds.), The Proto-Andean Margin of Gondwana. Geological Society, London, Special Publications 142, pp. 259–281.
- Söllner, F., Leal, P.R., Miller, H., Brodtkorb, M.K. de, 2000. Edades U/Pb en circones de la riolacita de la Sierra de Ambargasta, provincia de Córdoba. In: Schalamuk, I., Brodtkorb M.K. de, Etcheverry, R. (Eds.), Mineralogía y Metalogenia. INREMI, La Plata, Publicación 6, pp. 465–469.
- Sparisci, O., de Brodtkorb, M.K., 1998. Los diques lamprofíricos de Santo Domingo, provincia de San Luis, Argentina. 10º Congreso Latinoamericano de Geología y 6º Congreso Nacional de Geología Económica, Actas II, 201–204.
- Steiger, R.H., Jäger, E., 1977. Subcommission on geochronology: convention on the use of decay constants in geochronology and cosmochronology. Contributions to the geologic time scale. Studies in Geology 6, 67–72.
- Streckeisen, A., 1979. Classification and nomenclature of volcanic rocks, lamprophyres, carbonatites and melilitic rocks: recommendations and suggestions for the IUGS subcommission on the subdivision of igneous rocks. Geology 7, 331–335.
- Sun, S.S., McDonough, W.F., 1989. Chemical and isotopic systematics of oceanic basalts; implications for mantle composition and processes. In: Saunders, A.D., Norry, M.J. (Eds.), Magmatism in the Ocean Basins. Geological Society, London, Special Publication 42, pp. 313–345.
- Suzuki, K., Shiraki, K., 1980. Chromite-bearing spessartites from Kasuga-Mura, Japan, and their bearing on possible mantle origin andesite. Contributions to Mineralogy and Petrology 71, 313–322.
- Tate, M.C., Clarke, D.B., 1993. Origin of the Late Devonian Weekend lamprophyre dykes, Meguma Zone, Nova Scotia. Canadian Journal of Earth Sciences 30, 2295–2304.
- Turpin, L., Velde, D., Pinte, G., 1988. Geochemical comparison between minettes and kersantites from the Western European Hercynian orogen: trace element and Pb-Sr-Nd isotope constraints on their origin. Earth and Planetary Science Letters 87, 73–86.
- Wilson, M., 1989. Igneous Petrogenesis: A Global Tectonic Approach. Chapman & Hall, London. p. 446.
- Wooley, A.R., Bergman, S.C., Edgar, A.D., Le Bas, M.J., Mitchell, R.H., Rock, N.M.S., Scott Smith, B.H., 1996. Classification of lamprophyres, lamproites, kimberlites, and the kalsilitic, melilitic and leucitic rocks. Canadian Mineralogist 34, 175–186.
- Zartman, R.E., Doe, B.R., 1981. Plumbotectonics – the model. In: Zartman, R.E., Taylor, S.R. (Eds.), Evolution of the Upper Mantle. Tectonophysics 75, pp. 135–162.
- Zindler, A., Hart, S.R., 1986. Chemical geodynamics. Annual Review Earth and Planetary Science 14, 493–571.